Remodeling of the Cortical Structural Connectome in Posttraumatic Stress Disorder: Results from the ENIGMA-PGC PTSD Consortium

Supplement

Supplementary Methods

Clinical Measurements

Most sites used clinician-administered measures such as the Structured Clinical Interview for DSM (SCID) (First, 2015) or Clinician-Administered PTSD Scale (CAPS) (Weathers et al., 2018; Weathers, Keane, & Davidson, 2001) to ascertain PTSD diagnosis. The majority used DSM-IV criteria, but a small subset of sites used DSM-5 criteria. Severity of PTSD symptoms was derived from the same measures used for diagnosis, except when a clinician-administered measure (e.g., SCID) lacked severity information (see **Supplementary Table S1**). The measures reflect PTSD diagnosis and symptoms in the month before scanning. Sites used a mix of clinician-administered and self-report instruments to diagnose depression. We harmonized depression data by assigning participants to major depressive disorder (MDD) or control groups based on a standardized depression severity cut-off score. Most sites reported depression severity using the Beck Depression Inventory-II (BDI-II) (Beck, Steer, & Brown, 1996), while other scales included the Center for Epidemiologic Studies Depression Scale (CES-D) (Radloff, 1977), Hamilton Depression Rating Scale (HAM-D) (Hamilton, 1980), Depression Anxiety Stress Scales (DASS) (Lovibond & Lovibond, 1995), and Children's Depression Inventory (CDI) (Kovacs, 1985).

Imaging Data Preprocessing

Anatomical brain images were preprocessed at Duke University with a standardized neuroimaging and QC pipeline developed by the ENIGMA Consortium (http://enigma.ini.usc.edu/protocols/imaging-protocols/) (Wang et al., 2020). CT and SA measurements were generated by FreeSurfer software (https://surfer.nmr.mgh.harvard.edu) based on the Destrieux atlas (Destrieux, Fischl, Dale, & Halgren, 2010) that contains 74 regions per hemisphere. In brief, white matter surfaces were deformed toward the gray matter boundary at each surface vertex. CT was calculated based on the average distance between the parcellated portions of white and pial surfaces within each region, and SA was measured as the area within each region. The CT and SA estimates for each region and subject were entered into further respective analyses. The quality of structural images per hemisphere from each site (in 21 of 29 sites) was assessed with the Euler number, which is a measure of topological complexity of the reconstructed cortical surface (Rosen et al., 2018). As shown in **Supplementary Table S3**, the Euler number did not show significant difference between PTSD and non-PTSD groups at most sites except for Duke University (DeBellis) and INTRUST.

Harmonizing Data Across Sites

ComBat achieves harmonization by first modeling expected imaging features as linear combinations of the biological variables and site effects whose error term is further modulated by site-specific scaling factors. Secondly, *ComBat* applies empirical Bayes to improve the estimation of site parameters for small samples. This method effectively removes unwanted sources of site variability thereby increasing the power and reproducibility of subsequent statistical analyses of multi-site studies on CT (Radua et al., 2020; D. Sun et al., 2021). PTSD diagnosis, age, and sex were designated as biological variables, but PTSD severity and

depression diagnosis were not designated as biological variables because they were highly correlated with PTSD diagnosis, and some participants were missing information on PTSD severity and depression.

Adjusting for Confounding Factors

We did not include sex as a regressor for the investigation of the interaction between sex and PTSD diagnosis. Similarly, we did not include age and age^2 as regressors for the investigation of age effects on PTSD diagnosis. We then entered the residuals of the linear model into the following analyses.

Replication Analyses

To test the reliability of our results comparing actual networks to random networks in the PTSD group, non-PTSD group, and PTSD versus non-PTSD, we conducted 5,000 iterations of leaving out three sites to calculate the 95% confidence interval of mean SC for each type of network. For each iteration, we randomly removed 3 out of 29 sites (~10% of all sites) and performed the same analyses on the remaining data including data harmonization, adjustment for covariates, calculation of the mean SC of the actual network with top-*n* regions for the PTSD group, non-PTSD group, and the between-group comparison as described above. Our approach is more robust than performing a split sample reproducibility test, which may lead to a false confirmation or a false rejection of results. Removing three sites is superior to removing a single site at each iteration given that some of the sites have relatively small sample sizes, which may also produce spurious results.

Global and Individual Tests

We performed two tests of statistical significance that were complementary to each other – the global test and the individual test. The mean SC between *n*-regions was plotted as a function of *n* (from *n* = 2 to 148; **Fig. 1C**). As implemented by Wannan et al. (2019), the area under this curve (AUC) was used to compute the *p*-value for the global test, which was the proportion of AUC values from the randomly generated networks of *n*-regions that exceeded or equaled the AUC values for the actual networks of top-*n* regions. The *p*-value for the individual test was calculated for each value of *n* as the proportion of mean SC values from randomly chosen sets of *n* regions that exceeded or equaled the mean SC from the actual top-*n* network. The global *p*-value gives an overall estimate of the connections regardless of network size, while the individual *p*-value reflects how connections are influenced by the size of cortical networks. Both global and individual *p*-values were derived from two-tailed tests.

Corrections for Multiple Comparisons

The Bonferroni method was employed to correct for the number of comparisons, i.e., 2 (CT-based and SA-based networks) by 3 (atrophic, hypertrophic, and stable networks), in global tests and individual tests. This method was also employed to correct for the 6 comparisons (i.e., all pairs among 4 subgroups) where there was a significant interaction between PTSD diagnosis and depression, or sex, or age. The false discovery rate (FDR) method (Benjamini & Hochberg, 1995) was further employed in individual tests to correct for network size (totally 147, *n* = 2 to 148). All *p*-values shown are corrected for multiple comparisons.

Correlations Between Regional Average SC and Effect Size of Cortical Changes

To examine whether brain hubs that are strongly connected with other areas (Crossley et al., 2014), played a role in the spatial distribution of PTSD-related cortical changes, we investigated the association between the effect size of cortical changes for each region and the average of positive SC between said region and all the other cortical regions. This association was calculated by Pearson's correlation across regions separately in CT-based and SA-based networks in PTSD and non-PTSD groups.

Effects of PTSD Symptom Severity

To understand the influence of PTSD symptom severity on SCNs, we partitioned the sample into five ranges of very low (0 - 3), low (4 - 19), moderate (20 - 45), high (46 - 67), and very high (> 67) CAPS score (see **Supplementary Table S8**) with comparable sample sizes according to CAPS score quintiles. We were unable to directly analyze the effects of continuous measures of PTSD symptom severity because the mean SC was calculated for the whole group rather than for each participant. We investigated only participants with scores based on DSM-IV symptoms given their relatively large sample size (N = 1611), while omitting participants with DSM-5 symptoms scores. We examined the difference in mean SC by performing pairwise comparisons between all five groups.

Supplementary Results

Methodologic Confirmation of Rank Ordering

Actual versus Random Networks in PTSD. As displayed in **Fig. 3** and **Table 2**, global tests showed that PTSD patients had higher mean SC in CT-based ($p < 0.001$) and SA-based ($p = 0.017$) atrophic networks, CT-based ($p = 0.029$) and SA-based ($p = 0.017$) hypertrophic networks, and CT-based ($p < 0.001$), but not SA-based ($p > 0.5$) stable networks when compared to the corresponding random networks. No individual test results survived correction (*p-values* > 0.05). The results of this analysis serve as methodologic confirmation for selecting regions, which are rank-ordered by effect size, in forming SCNs of interest. The analysis of stable networks highlights this point most clearly. Although the stable regions individually differ the least between groups, the networks they form differ significantly in SC between group, except for SA-based stable SCNs.

Actual versus Random Networks in non-PTSD. As displayed in **Fig. 4** and **Table 2**, global tests showed that the non-PTSD participants had higher mean SC in CT-based ($p < 0.001$) and SA-based ($p < 0.001$) atrophic networks, in SA-based ($p = 0.014$), but not CT-based ($p = 0.139$) hypertrophic networks, and neither CT-based ($p = 0.264$) nor SA-based ($p = 0.732$) stable networks when compared to the corresponding random networks. Individual tests showed that the non-PTSD participants had higher mean SC in CT-based atrophic networks consisting of the top-69, 82, and 93 regions (*p-values* < 0.05), compared to the corresponding random networks. No other individual test results survived correction (*p-values* > 0.05). The results of this analysis serve as methodologic confirmation for selecting regions, which are rank-ordered by effect size, in the formation of *atrophic* SCNs of interest. Methodologic confirmation was achieved for SA-

based hypertrophic SCNs, but not for CT-based hypertrophic SCNs. Methodologic confirmation for stable SCNs was not achieved in the non-PTSD group.

Correlations between Regional Average SC and Effect Size of Cortical Changes

No significant correlation was found in CT-based (R = -0.091, p = 0.270) and SA-based (R = 0.021, p = 0.795) networks of patients with PTSD. No significant correlation was found in CT-based (R = -0.110, p = 0.183) and SA-based (R = -0.003, p = 0.967) networks of non-PTSD participants. These negative results suggest that the spatial distribution of PTSD-related cortical changes is not related to the brain hubs that are strongly connected to other areas (reflected by high SC between said region and all the other cortical regions), but are associated with the strength of connections among regions.

Effects of PTSD Symptom Severity. As displayed in **Supplementary Fig. S3**, global tests showed that, in the CT-based atrophic networks (**Supplementary Fig. S3A**), the low-severity group had greater mean SC than the very-low severity group (p < 0.001), and the high-severity group had greater mean SC than both the very low severity group (p < 0.001) and the very-high severity group (p = 0.048).

In the SA-based atrophic networks (**Supplementary Fig. S3B**), the very-low group has greater mean SC than the low group (p < 0.001), the high group (p < 0.001), and the very-high group (p < 0.001). The moderate group had greater mean SC than both the low group (p < 0.001) and the high group (p < 0.001). The very-high group had greater mean SC than the low group (p = 0.024) and the high group (p = 0.024).

In the CT-based hypertrophic networks (**Supplementary Fig. S3C**), the very-high group had greater mean SC than the very-low group (p < 0.001), the low group (p < 0.001), and the high

group ($p < 0.001$). The moderate group also had greater mean SC than the high group ($p < 0.001$).

In the SA-based hypertrophic networks (**Supplementary Fig. S3D**), the low group ($p = 0.048$), the moderate group ($p = 0.048$), the high group ($p < 0.001$), and the very-high group ($p = 0.024$) all had greater mean SC than the very-low group. The high group had greater mean SC than the low group ($p = 0.024$).

In the CT-based stable networks (**Supplementary Fig. S3E**), the very-low group had greater mean SC than the low group ($p < 0.001$), the moderate group ($p < 0.001$), the high group ($p < 0.001$), and the very high group ($p < 0.001$). The very high group had greater mean SC than the low group ($p < 0.001$).

In the SA-based stable networks (**Supplementary Fig. S3F**), the high group had greater mean SC than the very low group ($p < 0.001$).

Individual tests showed that very low group had greater mean SC compared to the low group in SA-based atrophic networks consisting of the top-72, 77 and 81 regions (*p-values* < 0.05). The low group had greater mean SC compared to the very low group in the SA-based hypertrophic networks consisting of the top-145 regions (*p-values* < 0.05). The high group had greater mean SC than the very low group in SA-based hypertrophic networks consisting of the top-119, 121-131, 133, 139, 140 and 142 regions (*p-values* < 0.05). No other between-group differences that were based on either global or individual tests survived correction (*p-values* > 0.05).

Supplementary Discussions

The cortical regions showing high SC with other regions may represent hubs in brain-network topology (Crossley et al., 2014). Indeed, we reported previously that PTSD is accompanied by altered CT estimates as well as differences in nodal centrality in some brain hubs (D. L. Sun, Haswell, Morey, & de Bellis, 2019), which is also supported by an earlier study by Mueller et al. (2015). However, we did not find a significant relationship between the effect size of PTSD-related CT (or SA) change in any given region and its average connections with all the other regions. Our findings suggest that PTSD-related cortical changes are shaped by brain networks with strong covariance, rather than hubs that are highly connected to other regions.

We explored how the PTSD-related differences in SCNs are modulated by sex and age, and whether the SCNs would be modulated by PTSD symptom severity. We found that (**Supplementary Fig. S1**), females with PTSD and males without PTSD had greater mean SC in CT-based atrophic networks than females without PTSD. Males without PTSD had greater mean SC in CT-based stable networks than males with PTSD and females without PTSD. We also found that (**Supplementary Fig. S2**) some participant groups exhibited an inverted U-shaped relationship between age and mean SC in CT-based atrophic networks (peaking in 20-30 year-old in participants without PTSD and 15-20 year-old patients with PTSD) and SA-based hypertrophic networks (peaking in 10-15 year-old participants for both groups). We found significant PTSD-related differences of mean SC in different age groups, particularly < 10 year-olds, as demonstrated by higher mean SC in CT-based hypertrophic and stable networks, lower mean SC in CT-based atrophic networks, and lower mean SC in SA-based hypertrophic networks. Our findings (**Supplementary Fig. S3**) showed that PTSD symptom severity is non-linearly associated with mean SC across various networks.

A previous study investigating the diffusion-based structural connectome in youth documented that males have stronger connections between modes associated with perception and

coordinated action, whereas females have stronger connections between analytical and intuitive processing modes (Ingalhalikar et al., 2014), demonstrating the sex-related differences in brain connections. We found that in non-PTSD participants, males have higher mean SC in the CT-based atrophic and stable networks than females. These results demonstrate, for the first time, that males and females have different networks to propagate PTSD-related cortical morphometric changes. Moreover, we found that PTSD versus non-PTSD females have higher mean SC in the CT-based atrophic networks, whereas PTSD versus non-PTSD males have lower mean SC in the CT-based stable networks. These results clearly highlight sex-differences in the cortical networks are modulated by PTSD. It is well known that females have higher risk of developing PTSD than males after exposure to a criterion-A traumatic event (Ramikie & Ressler, 2018). There are several potential explanations for sex differences in PTSD including the type of trauma experienced, the age at the time of trauma exposure, individual differences in perceptions of threat and loss of control, the levels of peritraumatic dissociation, social support, comorbid drugs and alcohol that may be used to regulate trauma-related symptoms, and the acute psychobiological reactions to trauma (Olff, Langeland, Draijer, & Gersons, 2007). Studies in recent years investigating specific brain regions and connections suggest that early trauma exposure is associated with a smaller limbic system and greater connectivity of salience hubs in males, whereas an enlarged amygdala and weaker connectivity of salience hubs in females (Helpman et al., 2017). Our findings of sex-related differences in SCNs may be associated with varying responses to traumatic experiences and the development of PTSD in males and females. Future longitudinal studies may help to further elaborate the associations between sex-specific brain network topography and elevated rates of PTSD.

The present study characterized trajectories of cortical networks across the life span with a cross-sectional analysis of eight developmental periods. A previous study by DuPre and Spreng (2017) on age-related SC based on grey matter volume in healthy individuals found: (1) an

inverted U-shaped relationship between age and SC peaking at around 40 years, and (2) a decline in SC strength over the life span. In the present study, PTSD and non-PTSD participants exhibited an inverted U-shaped relationship between age and mean SC in CT-based atrophic networks (peaking at 20-30 years in non-PTSD and 15-20 years in PTSD), and SA-based hypertrophic networks (peaking at 10-15 years in both PTSD and non-PTSD groups). These peaks in CT-based and SA-based networks appear much earlier than the peaks in grey matter structural networks reported by DuPre and Spreng (2017). There is no clear trend of CT-based or SA-based mean SC decline over the life span in either PTSD or non-PTSD participants. These differences suggest that the modulation of structural connections by age are determined by the type of morphometric measures. We found significant PTSD versus non-PTSD group differences in mean SC across different age groups, particularly age < 10 years, as signaled by higher mean SC in CT-based hypertrophic and stable networks, as well as lower mean SC in CT-based atrophic networks and SA-based hypertrophic networks. Our results suggest that multiple networks undergo transformation in a coordinated fashion to support the development of the brain as well as PTSD symptoms, particularly during early childhood.

Parallel network findings were observed between groups defined by DSM diagnosis of PTSD and groups formed based on PTSD symptom severity. Consistent with findings based on DSM diagnosis of PTSD that showed lower mean SC in SA-based atrophic networks, we found symptom severity groups in the low, high, and very-high ranges had lower mean SC in the SA-based atrophic networks than groups with symptom severity in the very low range. However, PTSD symptom severity is non-linearly associated with mean SC across various networks. The mean SC of some groups with intermediate symptom severity were beyond the range defined by the mean SC of groups with very-low and very-high symptom severity in CT-based and SA-based atrophic networks. These findings suggest that PTSD diagnosis and symptom severity share features in common, but are quite distinct in relation to cortico-cortical connections. While

PTSD diagnosis and symptom severity are strongly correlated, they are not equivalent since diagnosis of PTSD requires additional information such as the presence of a minimum number of symptoms from each symptom cluster. Therefore, while the relationship between PTSD symptom severity and SC is helpful to the interpretation of network topography, it does not supplant direct comparisons between diagnostic groupings. Moreover, the participants who had CAPS scores based on DSM-IV symptoms were only a subset of all participants in the present study. The findings derived from these participants may not be generalized to a much broader population.

Supplementary References

Beck, A. T., Steer, R. A., & Brown, G. K. (1996). *Manual for the Beck Depression Inventory-II*. San Antonio, TX: Psychological Corporation.

Benjamini, Y., & Hochberg, Y. (1995). Controlling the False Discovery Rate - a Practical and Powerful Approach to Multiple Testing. *Journal of the Royal Statistical Society Series B-Statistical Methodology, 57*(1), 289-300. doi:DOI 10.1111/j.2517-6161.1995.tb02031.x

Crossley, N. A., Mechelli, A., Scott, J., Carletti, F., Fox, P. T., McGuire, P., & Bullmore, E. T. (2014). The hubs of the human connectome are generally implicated in the anatomy of brain disorders. *Brain, 137*, 2382-2395. doi:10.1093/brain/awu132

Destrieux, C., Fischl, B., Dale, A., & Halgren, E. (2010). Automatic parcellation of human cortical gyri and sulci using standard anatomical nomenclature. *Neuroimage, 53*(1), 1-15. doi:10.1016/j.neuroimage.2010.06.010

DuPre, E., & Spreng, R. N. (2017). Structural covariance networks across the life span, from 6 to 94 years of age. *Network Neuroscience, 1*(3), 302-323. doi:10.1162/netn_a_00016

First, M. B. (2015). Structured Clinical Interview for the DSM (SCID). In R. L. C. a. S. O. Lilienfeld (Ed.), *The Encyclopedia of Clinical Psychology* (pp. 1-6).

Hamilton, M. (1980). Rating Depressive Patients. *Journal of Clinical Psychiatry, 41*(12), 21-24.

Helpman, L., Zhu, X., Suarez-Jimenez, B., Lazarov, A., Monk, C., & Neria, Y. (2017). Sex Differences in Trauma-Related Psychopathology: a Critical Review of Neuroimaging Literature (2014-2017). *Current Psychiatry Reports, 19*(12). doi:ARTN 104

10.1007/s11920-017-0854-y

Ingalhalikar, M., Smith, A., Parker, D., Satterthwaite, T. D., Elliott, M. A., Ruparel, K., . . . Verma, R. (2014). Sex differences in the structural connectome of the human brain. *Proceedings of the National Academy of Sciences of the United States of America, 111*(2), 823-828. doi:10.1073/pnas.1316909110

Kovacs, M. (1985). The Children's Depression, Inventory (CDI). *Psychopharmacol Bull, 21*(4), 995-998.

Lovibond, P. F., & Lovibond, S. H. (1995). The structure of negative emotional states: comparison of the Depression Anxiety Stress Scales (DASS) with the Beck Depression and Anxiety Inventories. *Behav Res Ther, 33*(3), 335-343. doi:10.1016/0005-7967(94)00075-u

M., H. (1960). A rating scale for depression. *Journal of Neurology, Neurosurgery and Psychiatry, 23*, 56-62.

Mueller, S. G., Ng, P., Neylan, T., Mackin, S., Wolkowitz, O., Mellon, S., . . . Weiner, M. W. (2015). Evidence for disrupted gray matter structural connectivity in posttraumatic stress disorder. *Psychiatry Research-Neuroimaging, 234*(2), 194-201. doi:10.1016/j.pscychresns.2015.09.006

Olff, M., Langeland, W., Draijer, N., & Gersons, B. P. R. (2007). Gender differences in posttraumatic stress disorder. *Psychological Bulletin, 133*(2), 183-204. doi:10.1037/0033-2909.133.2.183

Radloff, L. S. (1977). The CES-D scale: A self report depression scale for research in the general population. *Applied Psychological Measurements, 1*, 385-401.

Radua, J., Vieta, E., Shinohara, R., Kochunov, P., Quide, Y., Green, M. J., . . . collaborators, E. C. (2020). Increased power by harmonizing structural MRI site differences with the ComBat batch adjustment method in ENIGMA. *Neuroimage, 218*, 116956. doi:10.1016/j.neuroimage.2020.116956

Ramikie, T. S., & Ressler, K. J. (2018). Mechanisms of Sex Differences in Fear and Posttraumatic Stress Disorder. *Biological Psychiatry, 83*(10), 876-885. doi:10.1016/j.biopsych.2017.11.016

Rosen, A. F. G., Roalf, D. R., Ruparel, K., Blake, J., Seelaus, K., Villa, L. P., . . . Satterthwaite, T. D. (2018). Quantitative assessment of structural image quality. *Neuroimage, 169*, 407-418. doi:10.1016/j.neuroimage.2017.12.059

Sun, D., Rakesh, G., Haswell, C. C., Logue, M., Lexi Baird, C., O'Leary, B. M., . . . Morey, R. A. (2021). A Comparison of Methods to Harmonize Cortical Thickness Measurements Across Scanners and Sites. *bioRxiv*, 2021.2009.2022.461242. doi:10.1101/2021.09.22.461242

Sun, D. L., Haswell, C. C., Morey, R. A., & de Bellis, M. D. (2019). Brain structural covariance network centrality in maltreated youth with PTSD and in maltreated youth resilient to PTSD. *Development and Psychopathology, 31*(2), 557-571. doi:10.1017/S0954579418000093

Wang, X., Xie, H., Chen, T., Cotton, A. S., Salminen, L. E., Logue, M. W., . . . Liberzon, I. (2020). Cortical volume abnormalities in posttraumatic stress disorder: an ENIGMA-psychiatric genomics consortium PTSD workgroup mega-analysis. *Molecular Psychiatry*. doi:10.1038/s41380-020-00967-1

Weathers, F. W., Bovin, M. J., Lee, D. J., Sloan, D. M., Schnurr, P. P., Kaloupek, D. G., . . . Marx, B. P. (2018). The Clinician-Administered PTSD Scale for DSM-5 (CAPS-5): Development and initial psychometric evaluation in military veterans. *Psychol Assess, 30*(3), 383-395. doi:10.1037/pas0000486

Weathers, F. W., Keane, T. M., & Davidson, J. R. (2001). Clinician-administered PTSD scale: a review of the first ten years of research. *Depression and Anxiety, 13*(3), 132-156. doi:10.1002/da.1029

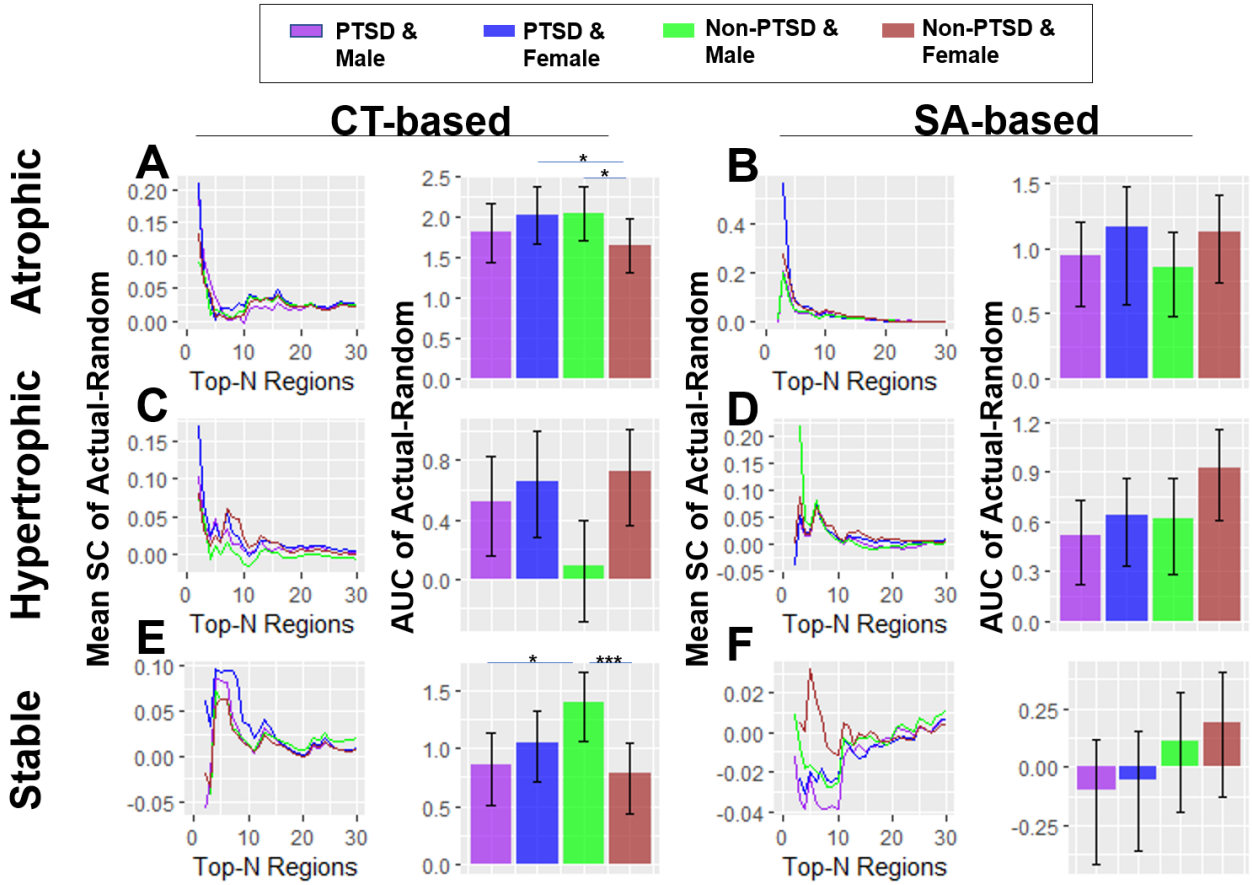

Supplementary Figure S1. Effects of PTSD x sex interaction. Global tests showed that (A) females with PTSD (p = 0.029) and males without PTSD (p = 0.014) had greater mean SC in CT-based atrophic networks than females without PTSD. (E) males without PTSD had greater mean SC in CT-based stable networks than males with PTSD (p = 0.014) and females without PTSD (p < 0.001). No significant PTSD x sex interaction effect (global p-values > 0.1) was found in the other types of networks shown in (B), (C), (D) and (F). The curves of networks with up to 30 nodes were shown for illustrative purpose. Error bar denotes 95% confidence interval of 5,000 random networks. *, p < 0.05; ***, p < 0.001.

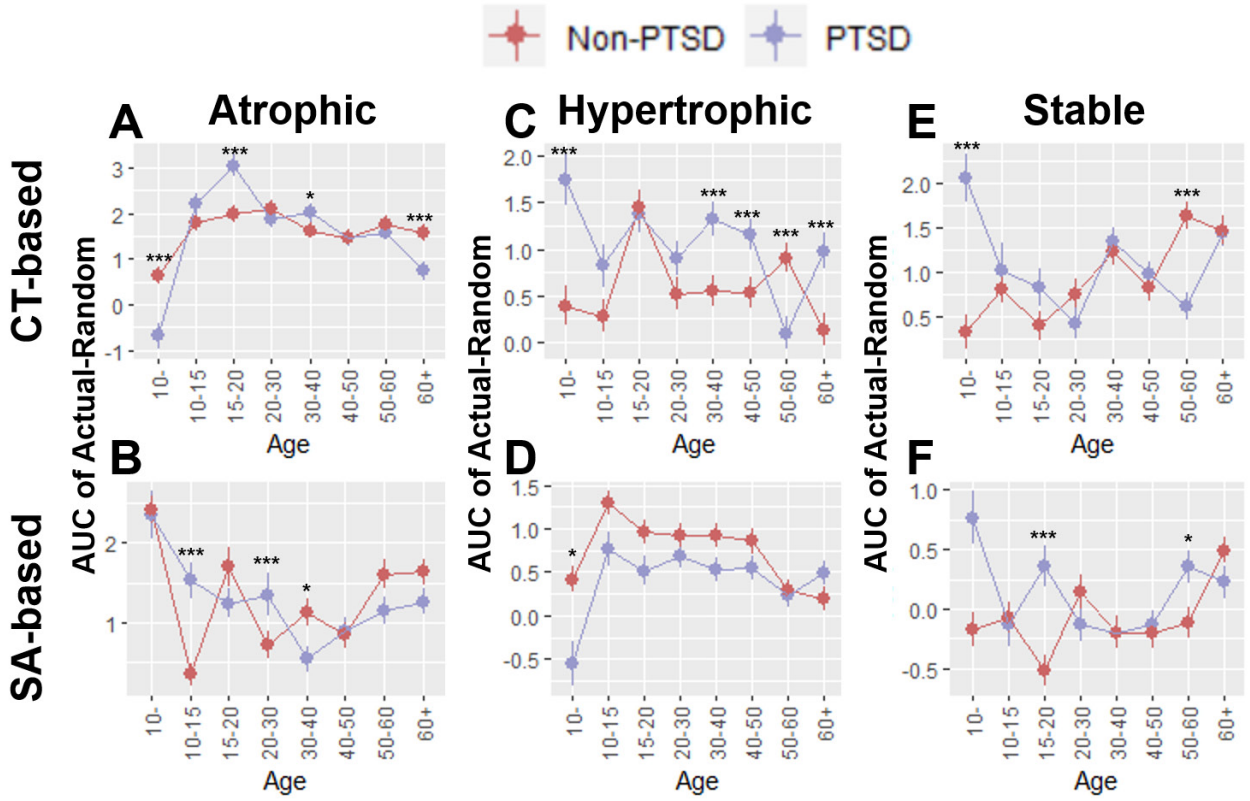

Supplementary Figure S2. Effects of PTSD x age interaction. An inverted-U relationship between age and mean SC was observed in (A) CT-based atrophic networks in both non-PTSD participants (peaking at 20-30 years old) and PTSD patients (peaking at 15-20 years old), and (D) SA-based hypertrophic networks in PTSD patients and non-PTSD patients (both peaking at 10-15 years old). PTSD-related differences in mean SC were observed in different age groups, especially <10 years old, represented by (A) lower mean SC in CT-based atrophic networks (p < 0.001) and (D) SA-based hypertrophic networks (p = 0.019), as well as (C) higher mean SC in CT-based hypertrophic (p < 0.001) and (E) stable (p < 0.001) networks, in patients with PTSD compared to non-PTSD participants. We did not show the curves of mean SC per age group for simplicity. The curves of networks with up to 30 nodes were shown for illustrative purpose. Error bar denotes 95% confidence interval of 5,000 random networks. *, p < 0.05; ***, p < 0.001.

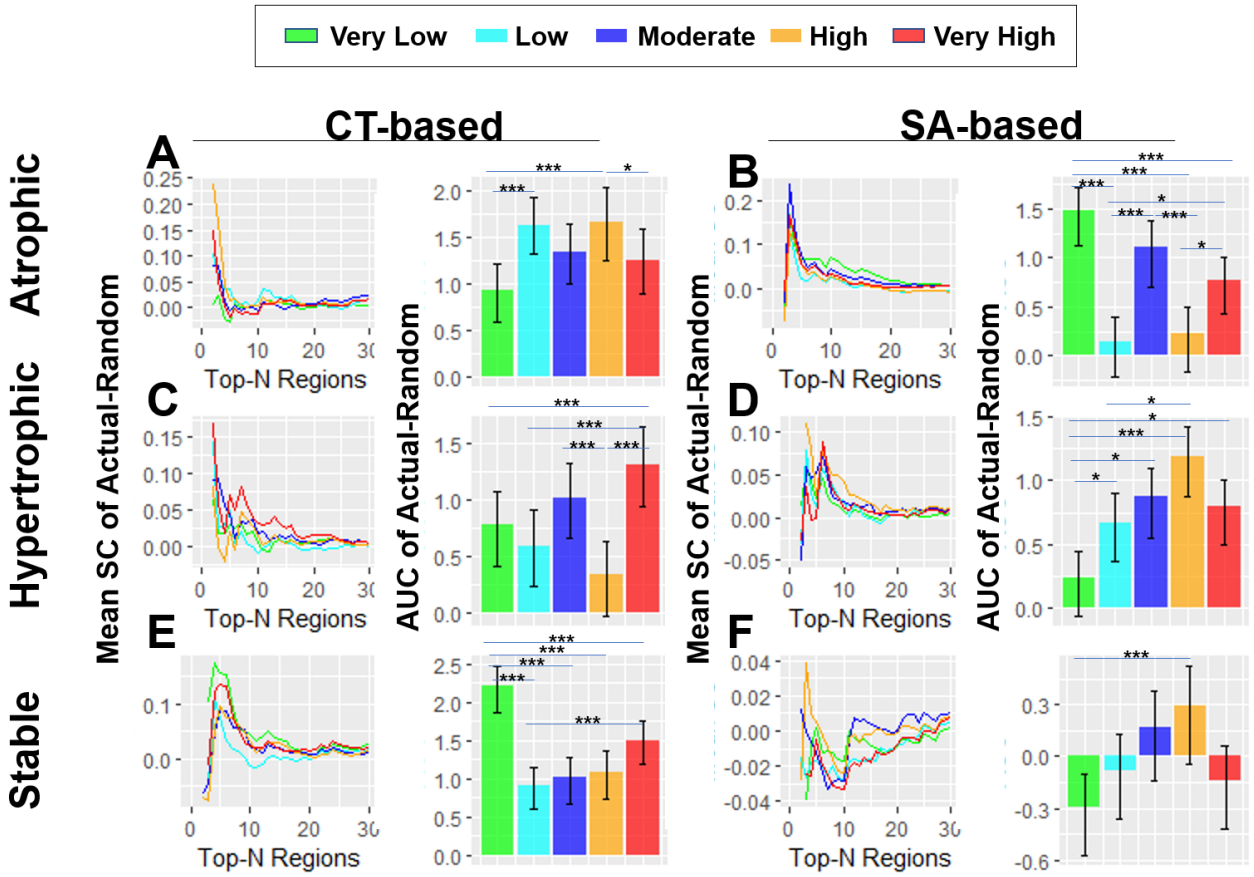

Supplementary Figure S3. Effects of PTSD symptom severity. Subgroups based on CAPS score: very low, 0-3; low, 4-19; moderate, 20-45; high, 46-67; very high, >67. The curves of networks with up to 30 nodes were shown for illustrative purpose. Error bar denotes 95% confidence interval of 5,000 random networks. *, $p < 0.05$; ***, $p < 0.001$.

Supplementary Table S1. Specific psychometric instruments per site.

Site	PTSD Tool	MDD Diagnoses Tool	Depression Symptom Severity Tool
Duke University	CAPS-4/CAPS-5/SCID	BDI-II	BDI-II
McLean	CAPS-5	BDI-II	BDI-II
Toledo	CAPS-4	MINI	DASS/CESD
West Haven	CAPS-4	SCID	BDI-II
Yale	CAPS-4	SCID	N/A
UCAS	PCL-5	CES-D	CES-D
ADNIDOD	CAPS-4	GDS	GDS
Emory GTP	CAPS-4/PSS	BDI-II	BDI-II
Stellenbosch	MINI/CAPS-5	N/A	N/A
Columbia	CAPS-4	HAMD	HAMD
Ghent	MINI	BDI-II	BDI-II
INTRUST	MINI/CAPS-4/PCL-M/SCID	PHQ9	PHQ9
UNSW	CAPS-4	HAMD	HAMD
Leiden	ADIS	CDI	CDI
University of Washington	DISC/CAPS-5/UCLA-PI	CDI	CDI
DUKE (DeBellis)	K-SADS-PL	N/A	N/A
Mannheim	SCID/DTS	BDI-II	BDI-II
University of Wisconsin-Madison	CAPS-4	BDI-II	BDI-II
Groningen	CAPS-4	BDI-II	BDI-II
Booster (AMC)	CAPS-4	HADS-D	HADS-D
McLean (Rosso)	CAPS-4	BDI-IA	BDI-IA
Stanford	CAPS-4	N/A	N/A
Minneapolis VA	CAPS-4	SCID	SCID
Muenster	SCID	BDI-II	BDI-II
WACO VA	PCL-5	BDI-II	BDI-II
University of Wisconsin-Milwaukee	CAPS-5	DASS	DASS
South Dakota	PCL-C / PCL-M	CES-D/BDI-II	CES-D/BDI-II
University of Illinois-Chicago	CAPS-4/PCL-M	BDI-II	BDI-II
University of Cape Town	MINI	BDI-II	BDI-II

Note: PTSD diagnostic tools: CAPS-4 (Clinician Administered PTSD Scale for DSM IV), MINI (Mini-International Neuropsychiatric Interview), CAPS-5 (CAPS for DSM-V), PSS (Posttraumatic Stress Scale), PCL-M (PTSD Checklist- Military), SCID (Structured Clinical Interview for DSM IV), PCL-C (PTSD Checklist- Civilian), PDS (Posttraumatic Diagnostic Scale), ADIS(Anxiety Disorder Interview Schedule), DTS(Davidson Trauma Scale). Childhood Trauma tools: CTQ (Childhood Trauma Questionnaire), TSCC (Trauma Symptom Checklist for Children), ETI (Early Trauma Inventory), SLESQ (Stressful Life Events Screening Questionnaire), TLEQ (Trauma Life

Events Questionnaire). Depression tools: GDS (Geriatric Depression Scale). HADS-D (Hospital Anxiety and Depression Scale-Depression), HAM-D (Hamilton Depression Scale), BDI (Beck Depression Inventory-II), PHQ-9 (Patient Health Questionnaire9), CESD (Center for Epidemiologic Studies Depression Scale), DASS 21 (Depression, Anxiety, Stress Scale-21 item short form), KSADS-PL (Schedule for Affective Disorders and Schizophrenia for School-Age Children--Present and Lifetime Version). Alcohol tool: AUDIT (Alcohol Use Disorders Identification Test), ASSIST (Alcohol, Smoking and Substance Involvement Screening Test).

Supplementary Table S2. MRI acquisition parameters.

(part I)

Site	Scanner	Model	Strength	Channel	Sequence	Voxel size (mm)
Duke University	GE	MR750	3T	8	FSPGR BRAVO	0.9375x0.9375x0.9375
	GE	EXCITE HD 3T	3T	8	FSPGR BRAVO	1 x 1 x 1
	GE	4T LX Nvi	4T	8	Spin-echo co-planar	1x1x1.9
	Philips	Ingenia	3T	8	3D TFE SENSE	0.9375x0.9375x1
McLean	Siemens	Trio	3T	12	MEMPRAGE tfl_mgh_multiecho	1x1x1
Toledo	GE	SignaX	3T	8	SPGR	1x1x1
West Haven	Siemens	Tim Trio	3T	12	MPRAGE	1x1x1
Yale	Siemens	Tim Trio	3T	32	MPRAGE	1x1x1
UCAS	Philips	Achieva	3T	8	EPI	1x1x1
ADNIDOD	GE	GE Discovery MR750w	3T	40	FSPGR	1x1x1.2
	GE	GE Signa HDxt	3T	8	SPGR	1x1x1.2
	Siemens	Siemens TrioTim	3T	12	MPRAGE	1x1x1.2
	GE	GE Discovery MR750w	3T	8	SPGR	1x1x1.2
Emory GTP	Siemens	TIM Trio	3T	12	MPRAGE	1x1x1
Stellenbosch	Siemens	Allegra	3T	4	MPRAGE	1x1x1
	Siemens	Skyra	3T	32	MPRAGE	1x1x1
Columbia	GE	SIGNA EXCITE	1.5T	8	SPGR	3.5X3.5X2.2
Ghent	Siemens	TimTrio	3T	32	MPRAGE	1x1x1
INTRUST	GE	multiple	3T	8	SPGR-BRAVO	1x1x1
	Siemens	multiple	3T	12	MPRAGE	1x1x1
	Philips	multiple	3T	8	T1W_3D_TFESENSE	1x1x1
UNSW	GE	Signa Hdx	3T	8	3D SPGR	1x1x1
Leiden	Philips	Achieva	3T	8	gradient echo T1-weightedEPI	1.17x1.17x1.2
University of Washington	Siemens	Tim Trio	3T	32	MEMPRAGE	1x1x1
	Philips	Achieva	3T	32	MEMPRAGE	1x1x1
DUKE (DeBellis)	Siemens	Tim Trio	3T	8	MEMPRAGE	1x1x1
Mannheim	Siemens	Trio	3T	32	SPGR	1x1x1
University of Wisconsin-Madison	GE	X750 Discovery	3T	8	BRAVO	1x1x1
Groningen	Siemens	TrioTim	3T	12	MPRAGE	1x1x1
Booster (AMC)	Philips	Achieva	3T	32	FAST MPRAGE	1x1x1

McLean (Rosso)	Siemens	Tim Trio	3T	32	MEMPRAGE	1.3X1X1.3
Stanford	GE	MR750	3T	8	3D SPGR	1.5x0.9x1.1
Minneapolis VA	Siemens	TimTrio	3T	12	MPRAGE	1x1x1
Muenster	Siemens	Magnetom Prisma	3T	20	MPRAGE	1x1x1
WACO VA	Philips	Achieva	3T	16	MPRAGE	1x1x1
Univ of Wisconsin-Milwaukee	GE	MR750 Signa Excite	3T	32	SPGR	1x0.9375x0.9375
South Dakota	Siemens	Skyra	3T	20	MPRAGE	1x1x1
University of Illinois-Chicago	GE	Signa	3T	8	Gradient-echo spiral pulse	1x1x1
University of Cape Town	Siemens	Skyra	3T	4	MPRAGE	1x1x1.5
	Siemens	Allegra	3T	4	MPRAGE	1x1x1.5

(part II)

Site	FOV (mm)	Acquisition Orientation	TR (ms)	TE (s)	Flip Angle	Slice Thickness (mm)	FreeSurfer Version
Duke University	256x256	Axial	8160	3.2	12	1	5.3
	240x240	Axial	8148, 7840, 8160	3.2, 2.9, 3.2	12	1	5.3
	240x240	Axial	12000	5.4	20	2	5.3
	240x240	Axial	8148	3.7	8	1	5.3
McLean	256	Sagittal	2530	1.64, 3.5, 5.36, 7.22	7	1	5.3
Toledo	256x256	Axial	7.9	3	9	1	5.3
West Haven	256x256	Sagittal	2530	2.71	7	1	5.3
Yale	256x256	Sagittal	2500	2.77	7	1	5.3
UCAS	220X220	Axial	8.5	3.7	8	2	5.3
ADNIDOD	256x256	Sagittal	7.652	3.104	11	1.2	6
	256x256	Sagittal	6.984	2.848	11	1.2	6
	256x255	Sagittal	2300	2.98	9	1.2	6
	256x256	Sagittal	7.34	3.036	11	1.2	6
Emory GTP	224x256	Axial	2600	3	8	1	5.3
Stellenbosch	256x256	Sagittal	2530	1.5, 3.2, 4.9, 6.6	7	1	5.3
	280x280	Sagittal	2530	1.63, 3.47, 5.31, 7.15	7	1	5.3
Columbia	224X224	Axial	3000	30	84	2.2	5.3
Ghent	256x256	Transversal	2250	4.18	9	1	5.3
INTRUST	256x256	Sagittal	9150	3.7	10	1	5.3
	256x256	Sagittal	2530	3.32	7	1	5.3

	256x256	Sagittal	7,600	3.5	7	1	5.3
UNSW	256x256	Sagittal	8,300	3.24	11	1	5.3
Leiden	224x177x168	Sagittal	9.8	4.6	8	1.2	5.3
University of Washington	220x220	Sagittal	2530	1.6-7	7	1	5.3
	256x256	Sagittal	2530	3.5	7	1	5.3
DUKE (DeBellis)	256x256x124	Axial	1750	5.17	20	1	5.3
Mannheim	192x192	Axial	2000	3	80	3	5.3
University of Wisconsin-Madison	256x256	Axial	8.16	3.18	12	1	5.3
Groningen	256X256	Sagittal	1900	2.5	9	1	5.3
Booster (AMC)	240x188	Axial	8200	3800	8	1	5.3
McLean (Rosso)	256X128	Sagittal	2530	3.31	7	1.33	5.3
Stanford	220X220, 240x240	Coronal	8, 8.6	3.6, 3.4	15	1.1	5.3
Minneapolis VA	256X256	Coronal	2530	3.7	7	1	6
Muenster	256	Sagittal	3240	2.28	8	1	5.3
WACO VA	288x288	Sagittal	2400	3.08	90	1	6
Univ of Wisconsin-Milwaukee	240	Sagittal	8.2	3.2	12	1	5.3
South Dakota	240x240x180, 256x256x256	Sagittal, interleaved	1900	2.13	9	0.9	5.3
University of Illinois-Chicago	240x240	Coronal	25	6.6	90	1	5.3
University of Cape Town	256x256	Sagittal	2530	1.69, 3.55, 5.41, 7.27	7	1.5	5.3
	256x256	Sagittal	2000	1.53, 3.21, 4.89, 6.57	20	1.5	5.3

Note: FOV=field of view, TR=repetition time, TE=echo time, T=Tesla, FSPGR=fast spoiled gradient echo, BRAVO = brain volume, TFE=turbo field echo, SENSE=sensitivity encoding, MEMPRAGE=multi-echo MPRAGE, MPRAGE=magnetization prepared rapid gradient echo, TFL=tensor fascia lata, MGH=Massachusetts General Hospital, SPGR=spoiled gradient echo, EPI=echo planar.

Supplementary Table S3. Euler number (mean±SD) per hemisphere.

	Left Hemisphere				Right Hemisphere			
Site	**PTSD**	**non-PTSD**	***t***	***p***	**PTSD**	**non-PTSD**	***t***	***p***
ADNIDOD	-	-	-	-	-	-	-	-
Booster (AMC)	-19.2 ±12.7	-18.3 ±8.7	-0.364	0.717	-19.7 ±9.8	-17.4 ±8.7	-1.064	0.291
Columbia	-751.5 ±360.4	-666.7 ±312.8	-1.122	0.265	-778.8 ±357.1	-723.2 ±313.0	-0.740	0.461
Duke University (DeBellis)	-483.9 ±355.5	-322.0 ±144.4	-3.504	0.001**	-511.2 ±424.2	-327.5 ±140.9	-3.536	0.001**
Minneapolis VAMC	-111.9 ±56.9	-106.2 ±46.2	-0.709	0.480	-121.7 ±60.3	-116.7 ±53.4	-0.572	0.568
Duke University /Durham VA	-173.4 ±86.8	-155.5 ±86.5	-1.701	0.090	-165.6 ±79.5	-154.2 ±81.0	-1.168	0.244
Ghent	-29.5 ±17.8	-38.1 ±16.6	1.359	0.179	-37.5 ±25.0	-35.5 ±12.6	-0.363	0.718
Groningen (Charité Berlin)	-	-	-	-	-	-	-	-
University of Wisconsin (Grupe)	-168.4 ±67.5	-159.2 ±70.6	-0.472	0.639	-145.9 ±57.8	-148.0 ±44.8	0.153	0.879
Emory GTP	-40.2 ±18.9	-35.8 ±18.1	-1.174	0.243	-35.4 ±22.0	-34.0 ±18.1	-0.353	0.725
INTRUST	-98.3 ±89.6	-79.8 ±47.4	-2.586	0.010*	-100.0 ±58.7	-82.8 ±43.5	-3.191	0.002**
University of Wisconsin (Larson)	-128.4 ±103.9	-112.1 ±90.8	-0.645	0.521	-119.6 ±83.6	-125.3 ±101.0	0.221	0.826
Leiden	-	-	-	-	-	-	-	-
Mannheim	-	-	-	-	-	-	-	-
McLean	-38.9 ±16.5	-41.7 ±22.7	0.465	0.644	-36.0 ±11.8	-42.2 ±19.4	1.344	0.185
Muenster	-38.2 ±17.6	-41.5 ±17.4	0.652	0.518	-35.6 ±12.3	-33.6 ±15.6	-0.480	0.633
Phan	-126.7	-127.2	0.029	0.977	-119.0	-132.4	1.100	0.278

	±52.4	±60.9			±33.7	±46.2		
McLean (Rosso)	-25.6 ±17.2	-28.8 ±12.4	0.941	0.349	-29.2 ±13.1	-30.2 ±14.3	0.287	0.775
University of Toledo	-	-	-	-	-	-	-	-
UCAS	-25.9 ±11.0	-30.3 ±15.0	1.345	0.183	-23.3 ±12.3	-26.3 ±15.3	0.871	0.387
Cape Town	-	-	-	-	-	-	-	-
University of Washington	-111.3 ±40.1	-110.9 ±57.0	-0.034	0.973	-108.3 ±46.4	-103.9 ±60.2	-0.382	0.703
WACO VA	-73.6 ±41.0	-65.5 ±38.6	-0.774	0.442	-73.8 ±44.6	-65.0 ±31.2	-0.844	0.402
WestHaven VA	-36.4 ±23.9	-32.4 ±14.3	-0.774	0.442	-31.0 ±17.8	-28.3 ±16.6	-0.602	0.550
Yale	-42.8 ±23.9	-39.2 ±22.1	-0.612	0.543	-38.6 ±22.5	-34.4 ±14.5	-0.945	0.348
UNSW	-	-	-	-	-	-	-	-
South Dakota	-84.6 ±53.6	-77.1 ±38.5	-0.832	0.407	-81.0 ±75.0	-73.9 ±38.4	-0.596	0.552
Stellenbosch	-	-	-	-	-	-	-	-
Stanford	-66.4 ±48.8	-100.0 ±0.0	0.683	0.497	-58.7 ±44.0	-66.0 ±0.0	0.165	0.870

Note: *, $p < 0.05$; **, $p < 0.01$; ***, $p <= 0.001$ for t tests; -, data unavailable.

Supplementary Table S4. Cortical regions rank ordered by effect size of PTSD-related differences in cortical thickness (CT) and surface area (SA).

Cortical Thickness (CT)						Surface Area (SA)					
	PTSD		Non-PTSD		Effect Size		PTSD		Non-PTSD		Effect Size
Area	M	SD	M	SD		Area	M	SD	M	SD	
R_G_temp_sup-Plan_polar	3.1	0.3	3.2	0.3	-0.103	L_S_orbital-H_Shaped	953.3	148.5	969.8	151.5	-0.110
R_S_circular_insula_inf	2.7	0.2	2.7	0.2	-0.098	R_S_circular_insula_inf	813.9	99.4	823.0	103.5	-0.090
R_G_oc-temp_med-Parahip	3.0	0.2	3.1	0.3	-0.078	R_S_orbital-H_Shaped	978.2	154.0	993.4	160.0	-0.086
R_G_and_S_occipital_inf	2.5	0.2	2.5	0.2	-0.074	R_S_central	2090.6	247.1	2106.7	240.3	-0.067
L_G_temp_sup-Plan_tempo	2.5	0.2	2.5	0.2	-0.071	L_S_cingul-Marginalis	763.6	110.4	772.8	109.5	-0.066
R_G_temp_sup-Lateral	3.0	0.2	3.0	0.2	-0.071	L_G_subcallosal	336.5	126.5	345.1	130.8	-0.063
L_G_Ins_lg_and_S_cent_ins	3.1	0.3	3.2	0.3	-0.065	L_S_circular_insula_inf	959.5	110.4	967.2	114.7	-0.062
L_G_occipital_middle	2.4	0.2	2.5	0.2	-0.064	L_S_orbital_med-olfact	542.9	108.6	551.7	110.7	-0.060
R_S_oc_middle_and_Lunatus	2.0	0.2	2.0	0.2	-0.061	R_G_and_S_cingul-Ant	1911.4	264.1	1930.6	266.0	-0.058
R_S_occipital_ant	2.3	0.2	2.3	0.2	-0.061	R_S_orbital_med-olfact	554.1	103.2	561.8	106.8	-0.057
L_S_circular_insula_inf	2.7	0.2	2.7	0.2	-0.060	L_S_oc_sup_and_transversal	863.5	153.3	876.1	159.5	-0.057
L_G_and_S_occipital_inf	2.3	0.2	2.3	0.2	-0.059	R_S_interm_prim-Jensen	320.5	135.3	329.5	138.4	-0.055
R_G_pariet_inf-Supramar	2.6	0.2	2.7	0.2	-0.056	L_S_precentral-inf-part	1039.2	186.6	1053.6	195.5	-0.053
R_G_Ins_lg_and_S_cent_ins	3.2	0.3	3.3	0.3	-0.055	L_G_and_S_frontomargin	821.0	120.8	829.8	123.6	-0.053
L_G_rectus	2.5	0.2	2.5	0.2	-0.053	L_G_temp_sup-Lateral	1400.3	184.7	1412.8	183.1	-0.052

L_S_oc_middle_and_Lunatus	1.9	0.2	2.0	0.2	-0.052	R_S_calcarine	1666.5	288.9	1685.4	293.3	-0.050
L_G_temporal_inf	2.8	0.2	2.8	0.2	-0.048	R_S_occipital_ant	534.2	140.3	543.6	140.2	-0.048
R_G_oc-temp_lat-fusifor	2.8	0.2	2.8	0.2	-0.045	L_S_intrapariet_and_P_trans	2124.2	305.9	2145.9	303.8	-0.046
R_G_temporal_inf	2.8	0.2	2.8	0.2	-0.043	R_S_front_sup	1833.1	303.9	1853.7	307.2	-0.046
R_G_orbital	2.7	0.2	2.7	0.2	-0.043	L_S_occipital_ant	543.5	147.2	552.3	150.5	-0.044
R_S_oc_sup_and_transversal	2.1	0.1	2.1	0.1	-0.042	L_G_and_S_cingul-Mid-Post	927.6	120.7	934.8	127.6	-0.040
R_Pole_temporal	3.2	0.3	3.3	0.3	-0.041	L_S_front_middle	1054.1	228.4	1068.4	230.5	-0.038
R_G_oc-temp_med-Lingual	2.0	0.2	2.1	0.2	-0.041	R_G_pariet_inf-Angular	2006.4	330.6	2026.3	340.5	-0.038
R_G_parietal_sup	2.3	0.2	2.3	0.2	-0.040	L_G_occipital_sup	1033.7	160.2	1043.3	169.8	-0.038
R_G_precentral	2.7	0.2	2.7	0.2	-0.040	R_S_cingul-Marginalis	906.7	138.4	914.7	139.7	-0.036
L_S_intrapariet_and_P_trans	2.1	0.1	2.1	0.1	-0.040	L_S_parieto_occipital	1383.2	240.6	1395.0	241.7	-0.036
L_S_oc_sup_and_transversal	2.0	0.1	2.0	0.2	-0.039	L_G_insular_short	457.6	73.2	460.9	73.5	-0.035
L_G_and_S_paracentral	2.3	0.2	2.3	0.2	-0.039	L_G_front_middle	3065.1	508.1	3096.4	513.2	-0.034
L_S_temporal_sup	2.4	0.1	2.4	0.1	-0.038	R_G_occipital_middle	1536.8	263.3	1552.9	273.4	-0.033
R_S_postcentral	2.0	0.1	2.1	0.1	-0.037	R_S_pericallosal	998.6	192.5	1010.3	200.9	-0.032
R_G_insular_short	3.4	0.3	3.4	0.3	-0.037	L_S_postcentral	1962.0	305.3	1977.4	311.3	-0.030
L_G_pariet_inf-Supramar	2.7	0.2	2.7	0.2	-0.036	L_G_oc-temp_med-Parahip	836.5	155.5	842.9	150.8	-0.029
R_G_pariet_inf-Angular	2.6	0.2	2.6	0.2	-0.035	L_S_calcarine	1705.5	311.7	1720.2	306.4	-0.029

L_G_temp_sup-G_T_transv	2.4	0.2	2.4	0.2	-0.035	R_G_rectus	524.2	68.2	527.3	68.4	-0.027
R_S_orbital-H_Shaped	2.5	0.2	2.5	0.2	-0.033	L_G_and_S_cingul-Ant	1600.4	248.6	1613.4	246.3	-0.026
L_S_temporal_inf	2.4	0.2	2.4	0.2	-0.032	R_G_insular_short	427.5	84.9	430.4	82.3	-0.024
L_G_temp_sup-Lateral	3.0	0.2	3.0	0.2	-0.031	R_G_occipital_sup	1155.5	181.1	1164.4	190.0	-0.023
L_S_collat_transv_ant	2.6	0.3	2.6	0.3	-0.028	R_S_intrapariet_and_P_trans	2203.8	310.6	2218.4	308.3	-0.023
R_S_precentral-sup-part	2.3	0.2	2.3	0.2	-0.027	L_S_orbital_lateral	276.8	65.9	279.6	66.3	-0.023
L_G_orbital	2.7	0.2	2.7	0.2	-0.025	R_G_cingul-Post-ventral	201.5	47.2	203.2	47.2	-0.023
L_S_interm_prim-Jensen	2.3	0.4	2.3	0.4	-0.024	R_G_precuneus	1764.3	259.2	1778.5	275.6	-0.022
L_G_precentral	2.7	0.2	2.7	0.2	-0.024	L_S_pericallosal	752.0	155.6	760.6	164.7	-0.022
R_G_rectus	2.4	0.2	2.4	0.2	-0.023	R_S_oc_sup_and_transversal	1009.7	188.1	1018.0	190.4	-0.021
L_G_and_S_subcentral	2.6	0.2	2.6	0.2	-0.023	R_S_front_middle	1542.8	318.2	1556.1	314.9	-0.020
L_S_oc-temp_lat	2.4	0.2	2.4	0.2	-0.022	L_Lat_Fis-ant-Horizont	222.8	43.6	224.4	45.0	-0.019
L_G_insular_short	3.5	0.3	3.5	0.3	-0.022	R_G_and_S_frontomargin	683.2	99.2	687.6	96.8	-0.018
R_G_precuneus	2.5	0.2	2.5	0.2	-0.019	L_S_subparietal	747.3	165.3	754.3	174.7	-0.018
L_G_postcentral	2.1	0.2	2.1	0.2	-0.019	L_S_central	2157.7	244.8	2164.2	247.5	-0.016
L_S_temporal_transverse	2.4	0.3	2.4	0.3	-0.018	R_G_and_S_cingul-Mid-Ant	1036.7	150.6	1042.5	154.1	-0.016
L_S_orbital_med-olfact	2.3	0.2	2.3	0.2	-0.018	R_G_oc-temp_med-Parahip	946.2	176.0	950.9	184.1	-0.015
L_G_temp_sup-Plan_polar	3.3	0.3	3.3	0.3	-0.018	L_S_circular_insula_sup	1192.8	129.0	1198.8	132.6	-0.015
R_G_occipital_	2.5	0.2	2.5	0.2	-0.016	R_G_temp_s	1245.3	163.5	1252.3	169.7	-0.012

middle						up-Lateral					
L_S_postcentral	2.1	0.1	2.1	0.1	-0.016	R_S_collat_transv_ant	697.5	162.7	702.9	165.7	-0.011
R_G_temp_sup-Plan_tempo	2.5	0.2	2.5	0.2	-0.015	R_S_temporal_transverse	204.6	45.4	205.9	45.8	-0.010
R_S_collat_transv_post	2.1	0.2	2.1	0.2	-0.014	L_S_temporal_transverse	251.4	57.7	252.8	56.6	-0.009
L_S_central	1.9	0.1	1.9	0.1	-0.013	R_S_parieto_occipital	1501.1	256.4	1509.5	259.1	-0.009
R_G_and_S_transv_frontopol	2.5	0.2	2.5	0.2	-0.010	R_S_oc_middle_and_Lunatus	676.9	181.3	683.2	180.8	-0.009
L_S_collat_transv_post	2.0	0.2	2.1	0.2	-0.010	R_G_and_S_occipital_inf	897.0	159.3	901.4	164.3	-0.008
L_G_oc-temp_med-Parahip	3.0	0.3	3.0	0.3	-0.009	R_G_oc-temp_med-Lingual	1960.7	290.9	1970.2	300.0	-0.008
L_S_precentral-sup-part	2.4	0.2	2.4	0.2	-0.009	R_S_circular_insula_sup	947.1	118.5	951.3	119.8	-0.008
R_S_front_sup	2.4	0.2	2.4	0.2	-0.009	R_G_oc-temp_lat-fusifor	1302.7	249.4	1309.8	243.8	-0.008
L_S_occipital_ant	2.2	0.2	2.2	0.2	-0.009	R_G_temporal_middle	2021.0	282.8	2033.4	295.8	-0.007
L_G_parietal_sup	2.3	0.2	2.3	0.2	-0.007	L_G_and_S_cingul-Mid-Ant	970.7	158.9	975.8	164.5	-0.006
R_G_occipital_sup	2.1	0.2	2.1	0.2	-0.007	L_S_front_sup	2009.2	327.8	2020.8	324.6	-0.006
L_G_pariet_inf-Angular	2.6	0.2	2.6	0.2	-0.006	R_S_front_inf	1453.8	259.6	1463.1	253.1	-0.005
L_Lat_Fis-post	2.4	0.2	2.4	0.2	-0.006	R_S_subparietal	856.3	193.7	861.4	211.5	-0.005
R_S_central	1.9	0.1	1.9	0.1	-0.005	L_G_oc-temp_lat-fusifor	1281.1	232.8	1287.4	237.0	-0.005
L_G_temporal_middle	2.9	0.2	3.0	0.2	-0.005	L_G_orbital	1718.0	204.4	1725.2	208.5	-0.004
L_G_occipital_sup	2.1	0.2	2.1	0.2	-0.004	R_G_front_sup	4583.4	569.1	4607.9	581.4	-0.004

R_S_oc-temp_lat	2.5	0.2	2.5	0.2	-0.004	L_S_suborbital	457.6	85.3	458.8	85.1	-0.003
R_Pole_occipital	1.9	0.1	1.9	0.2	-0.003	L_S_front_inf	1613.7	282.1	1623.0	295.2	-0.003
R_G_cingul-Post-ventral	2.7	0.3	2.7	0.3	-0.002	L_G_cingul-Post-ventral	216.0	57.2	217.4	60.2	-0.002
L_G_oc-temp_lat-fusifor	2.7	0.2	2.7	0.2	-0.002	L_G_pariet_inf-Angular	1694.0	276.2	1702.7	281.5	0.000
R_S_temporal_sup	2.5	0.1	2.5	0.1	0.000	R_S_temporal_inf	866.1	196.3	871.2	207.4	0.000
L_S_front_inf	2.2	0.2	2.3	0.2	0.000	R_G_subcallosal	260.8	89.1	262.1	88.0	0.000
R_S_parieto_occipital	2.2	0.2	2.2	0.2	0.001	L_S_oc-temp_med_and_Lingual	1452.8	215.4	1458.4	226.7	0.001
L_S_parieto_occipital	2.2	0.2	2.2	0.2	0.001	R_G_orbital	1841.9	224.4	1849.6	222.8	0.001
R_S_intrapariet_and_P_trans	2.1	0.1	2.1	0.1	0.002	R_G_and_S_subcentral	924.5	135.4	928.3	143.6	0.003
L_S_pericallosal	2.2	0.3	2.2	0.3	0.002	R_G_cuneus	1439.4	215.8	1443.9	228.5	0.005
L_G_front_inf-Opercular	2.7	0.2	2.8	0.2	0.003	L_G_oc-temp_med-Lingual	2028.5	323.0	2035.2	328.8	0.005
L_Pole_occipital	1.9	0.2	1.9	0.2	0.005	L_S_oc_middle_and_Lunatus	757.8	178.6	760.7	177.9	0.007
L_S_oc-temp_med_and_Lingual	2.4	0.2	2.4	0.2	0.005	L_S_temporal_inf	981.7	230.1	985.5	226.6	0.007
R_S_circular_insula_ant	2.8	0.2	2.8	0.3	0.006	L_G_cingul-Post-dorsal	401.7	85.0	403.3	90.3	0.008
L_S_circular_insula_ant	2.8	0.2	2.8	0.3	0.006	L_Lat_Fis-post	808.1	123.0	810.5	129.2	0.008
L_G_precuneus	2.5	0.2	2.5	0.2	0.006	R_S_oc-temp_med_and_Lingual	1386.3	207.6	1390.0	204.4	0.008
L_Pole_temporal	3.2	0.3	3.2	0.3	0.007	L_S_temporal_sup	3850.5	525.8	3863.9	526.1	0.009
L_G_and_S_cingul-Mid-Post	2.6	0.2	2.6	0.2	0.008	L_G_parietal_sup	2010.5	331.6	2019.5	324.5	0.009
R_S_interm_pri	2.2	0.2	2.2	0.2	0.008	L_S_interm_p	245.2	122.5	245.5	122.3	0.009

m-Jensen						rim-Jensen					
R_S_suborbital	2.5	0.4	2.5	0.4	0.008	L_G_temporal_inf	1833.4	311.7	1840.3	322.6	0.010
R_G_postcentral	2.1	0.2	2.1	0.2	0.008	L_S_circular_insula_ant	351.7	62.0	352.7	62.2	0.011
R_G_cuneus	1.8	0.1	1.8	0.1	0.009	R_Pole_temporal	1205.7	143.8	1207.8	144.7	0.011
R_G_front_middle	2.6	0.2	2.6	0.2	0.009	R_G_front_middle	2780.5	460.6	2794.7	478.4	0.011
L_G_front_middle	2.6	0.2	2.6	0.2	0.010	L_G_precuneus	1788.6	280.2	1796.1	294.3	0.012
L_G_subcallosal	2.5	0.4	2.5	0.4	0.011	R_S_orbital_lateral	321.2	82.2	321.9	81.7	0.012
L_Lat_Fis-ant-Vertical	2.4	0.3	2.4	0.3	0.012	R_G_and_S_cingul-Mid-Post	1003.9	142.3	1006.8	146.0	0.013
L_Lat_Fis-ant-Horizont	2.2	0.3	2.3	0.3	0.013	R_G_postcentral	1381.6	208.8	1386.8	198.7	0.013
R_G_subcallosal	2.4	0.4	2.4	0.4	0.015	R_G_and_S_paracentral	883.0	131.5	885.1	126.3	0.015
L_G_and_S_cingul-Ant	2.7	0.2	2.7	0.2	0.017	R_S_precentral-sup-part	985.7	211.5	986.1	204.8	0.015
L_S_precentral-inf-part	2.4	0.2	2.4	0.2	0.017	L_G_Ins_lg_and_S_cent_ins	345.0	57.5	345.0	56.3	0.016
R_G_and_S_cingul-Ant	2.6	0.2	2.6	0.2	0.017	L_G_temporal_middle	1898.8	289.8	1906.1	298.1	0.016
L_S_suborbital	2.5	0.3	2.5	0.3	0.019	L_S_collat_transv_post	296.8	69.3	296.5	69.2	0.016
R_G_front_sup	2.8	0.2	2.8	0.2	0.021	L_G_front_inf-Orbital	229.5	56.4	229.5	58.2	0.018
R_G_temp_sup-G_T_transv	2.4	0.2	2.4	0.2	0.021	R_Lat_Fis-ant-Horizont	272.7	55.2	272.8	56.2	0.019
L_G_and_S_transv_frontopol	2.6	0.2	2.6	0.2	0.022	L_S_collat_transv_ant	670.5	162.4	671.3	164.7	0.020
L_G_cuneus	1.8	0.1	1.8	0.1	0.023	R_G_temp_sup-G_T_transv	274.3	57.6	274.6	56.6	0.020
R_S_oc-temp_med_and_	2.4	0.2	2.4	0.2	0.023	L_G_pariet_inf-Supramar	2006.4	329.6	2012.0	335.7	0.021

Lingual											
R_G_temporal_middle	3.0	0.2	3.0	0.2	0.026	R_S_postcentral	1691.2	306.1	1694.2	301.0	0.022
R_S_front_middle	2.1	0.2	2.1	0.2	0.026	L_G_postcentral	1516.7	222.3	1520.9	224.4	0.023
R_S_temporal_inf	2.5	0.2	2.5	0.2	0.027	L_G_temp_sup-G_T_transv	362.6	76.7	362.2	76.3	0.024
L_S_orbital_lateral	2.2	0.3	2.2	0.3	0.027	R_G_cingul-Post-dorsal	374.6	79.5	375.4	82.3	0.024
R_G_front_inf-Orbital	2.7	0.3	2.7	0.3	0.027	R_G_parietal_sup	1648.5	263.0	1651.5	263.4	0.025
L_G_and_S_cingul-Mid-Ant	2.7	0.2	2.7	0.2	0.029	R_G_front_inf-Orbital	254.1	57.7	253.3	57.7	0.027
L_G_and_S_frontomargin	2.3	0.2	2.3	0.2	0.029	L_G_temp_sup-Plan_tempo	692.1	148.3	692.0	146.6	0.027
R_S_calcarine	1.9	0.1	1.9	0.1	0.029	R_S_circular_insula_ant	409.0	76.7	408.8	74.2	0.028
R_G_and_S_cingul-Mid-Ant	2.7	0.2	2.7	0.2	0.030	L_Pole_temporal	1196.5	153.0	1196.0	152.1	0.028
R_G_and_S_subcentral	2.6	0.2	2.6	0.2	0.030	L_G_front_sup	4896.9	615.5	4908.2	614.2	0.031
L_G_front_inf-Orbital	2.8	0.3	2.8	0.3	0.031	R_S_oc-temp_lat	708.1	158.1	707.4	156.0	0.032
L_S_front_sup	2.4	0.2	2.4	0.2	0.031	R_G_precentral	1748.7	251.3	1749.7	258.6	0.032
R_G_and_S_paracentral	2.2	0.2	2.2	0.2	0.037	R_Lat_Fis-post	980.8	118.8	980.0	117.0	0.033
R_Lat_Fis-ant-Vertical	2.4	0.3	2.4	0.3	0.038	R_G_temporal_inf	1752.0	284.3	1753.0	294.5	0.033
R_G_cingul-Post-dorsal	2.9	0.2	2.9	0.2	0.041	L_G_and_S_occipital_inf	1114.3	195.2	1112.9	191.1	0.033
R_S_temporal_transverse	2.5	0.3	2.5	0.3	0.042	R_G_pariet_inf-Supramar	1829.5	307.0	1832.8	306.1	0.033
R_G_and_S_cingul-Mid-Post	2.6	0.2	2.6	0.2	0.043	L_Pole_occipital	1456.1	206.4	1454.9	210.9	0.035
L_G_front_sup	2.8	0.2	2.9	0.2	0.043	L_G_front_inf-Opercular	960.0	159.0	960.0	159.1	0.038
R_Lat_Fis-post	2.4	0.2	2.4	0.2	0.043	L_S_oc-temp_lat	650.8	146.1	649.4	150.3	0.039

R_G_front_inf-Opercular	2.7	0.2	2.7	0.2	0.046	R_G_front_inf-Triangul	740.4	162.0	738.0	159.5	0.041
R_S_precentral-inf-part	2.4	0.2	2.4	0.2	0.046	R_G_temp_sup-Plan_tempo	572.0	109.4	570.6	108.1	0.042
L_S_orbital-H_Shaped	2.6	0.2	2.6	0.2	0.047	L_G_and_S_transv_frontopol	494.8	90.5	493.5	93.1	0.044
R_S_circular_insula_sup	2.6	0.2	2.6	0.2	0.050	R_Lat_Fis-ant-Vertical	154.7	51.1	153.4	51.6	0.044
R_G_front_inf-Triangul	2.6	0.2	2.6	0.2	0.051	L_G_and_S_subcentral	1016.3	144.0	1015.9	150.0	0.044
R_S_orbital_med-olfact	2.2	0.2	2.2	0.2	0.052	L_G_cuneus	1348.4	221.9	1344.9	227.2	0.045
L_S_circular_insula_sup	2.6	0.2	2.6	0.2	0.052	R_S_temporal_sup	4174.0	561.8	4175.3	558.2	0.048
R_S_orbital_lateral	2.1	0.3	2.1	0.3	0.053	L_G_occipital_middle	1457.1	247.1	1454.6	249.7	0.055
R_Lat_Fis-ant-Horizont	2.2	0.2	2.2	0.2	0.053	L_G_rectus	689.9	84.4	688.4	83.6	0.056
L_G_cingul-Post-dorsal	2.9	0.2	2.9	0.2	0.056	R_G_Ins_lg_and_S_cent_ins	351.0	63.2	349.2	62.6	0.057
L_S_cingul-Marginalis	2.2	0.2	2.2	0.2	0.057	R_S_precentral-inf-part	1134.0	206.2	1129.0	202.1	0.058
L_S_calcarine	1.9	0.1	1.9	0.1	0.057	L_G_front_inf-Triangul	787.3	160.5	782.6	158.5	0.059
L_G_cingul-Post-ventral	2.4	0.3	2.4	0.3	0.057	R_S_collat_transv_post	355.2	99.9	351.4	97.2	0.060
L_G_oc-temp_med-Lingual	2.0	0.2	2.0	0.2	0.057	R_S_suborbital	226.9	75.4	223.2	77.4	0.061
R_G_and_S_frontomargin	2.3	0.2	2.3	0.2	0.058	R_Pole_occipital	2226.5	308.0	2217.7	312.6	0.064
R_S_collat_transv_ant	2.6	0.3	2.6	0.3	0.068	R_G_front_inf-Opercular	893.3	156.4	887.7	157.5	0.065
L_S_subparietal	2.3	0.2	2.3	0.2	0.074	R_G_and_S_transv_frontopol	788.2	142.2	782.9	140.9	0.069
R_S_pericallosal	2.2	0.3	2.2	0.3	0.079	L_G_precentral	1741.6	240.8	1736.4	240.0	0.072

R_S_cingul-Marginalis	2.3	0.2	2.3	0.2	0.080	L_G_and_S_paracentral	993.2	143.5	988.1	138.1	0.072
R_S_subparietal	2.4	0.2	2.4	0.2	0.082	L_Lat_Fis-ant-Vertical	206.2	61.8	203.0	60.0	0.073
L_G_front_inf-Triangul	2.6	0.2	2.6	0.2	0.087	L_G_temp_sup-Plan_polar	434.1	96.4	430.3	93.9	0.074
L_S_front_middle	2.2	0.2	2.2	0.2	0.103	L_S_precentral-sup-part	946.4	189.9	936.4	184.5	0.079
R_S_front_inf	2.2	0.2	2.2	0.2	0.112	R_G_temp_sup-Plan_polar	500.5	102.8	495.6	102.7	0.083

Note: Negative (positive) effect size represents lower (higher) CT and SA in patients with PTSD than non-PTSD participants. M = mean, SD = standard deviation, L = left, R = right, G = gyrus, S = sulcus.

Supplementary Table S5. Number of participants per subgroup for the analyses of PTSD x sex interaction.

	CT-based Network		SA-based Network	
	PTSD	non-PTSD	PTSD	non-PTSD
Male	725	1106	729	1102
Female	619	967	619	964

Supplementary Table S6. Number of participants per subgroup for the analyses of PTSD x age interaction.

	CT-based Network		SA-based Network	
	PTSD	non-PTSD	PTSD	non-PTSD
Age<10	27	64	26	66
10<=Age<15	40	138	41	138
15<=Age<20	49	148	49	148
20<=Age<30	347	550	348	545
30<=Age<40	375	420	377	416
40<=Age<50	251	358	252	360
50<=Age<60	143	235	143	233
Age>=60	112	160	112	160

Supplementary Table S7. Number of participants per subgroup for the analyses of PTSD x depression interaction.

	CT-based Network		SA-based Network	
	PTSD	non-PTSD	PTSD	non-PTSD
with depression	669	358	734	360
without depression	388	1370	396	1356

Supplementary Table S8. Number of participants per subgroup for the analyses of PTSD symptom severity.

	CT-based	SA-based
Very Low (CAPS<4)	282	280
Low (4<=CAPS<20)	282	279
Moderate (20<=CAPS<46)	300	293
High (46<=CAPS<68)	289	284
Very High (CAPS>=68)	292	293